2018

Performance Analysis of Internally Geared Positive Displacement Machines

Matthew Read
City University London, United Kingdom, matthew.read.3@city.ac.uk

Nikola Stosic
City University London, United Kingdom, n.stosic@city.ac.uk

Ian Smith
City University London, United Kingdom, i.k.smith@city.ac.uk

Port Flow Losses in Internally Geared Positive Displacement Machines

Matthew READ*, Ian SMITH, Nikola STOSIC

City, University of London,
Northampton Square, London, UK
Phone: +44 (0)20 7040 8746, Email: m.read@city.ac.uk

* Corresponding Author

ABSTRACT

Internally geared positive displacement machines consist of an externally lobed inner rotor rotating inside an internally lobed outer rotor. The rotors can have a constant profile along their length and rotate about parallel axes. Relative to the axis of rotation, the lobes of the rotors can either be straight (as found in conventional gerotor type machines), or helical (as previously proposed by the authors). In either case, the profiles must be specified in order to maintain continuous contact points between the rotors to maintain sealed working chambers. The use of stationary ported plates located at both end faces of the rotors enables periods when fluid is able to enter and leave the machine to be controlled. Shaping of the ports allows compression or expansion to occur within the working chambers formed by the lines of continuous contact between the two rotors. This paper explores the effects of geometrical parameters such as rotor profiles, helical rotor wrap angle and built-in volume ratio, on the losses that occur during filling and discharge of the working chamber for internally geared machines operating as compressors.

1. INTRODUCTION

Conventional twin screw machines consist of two externally lobed helical rotors, which rotate about parallel axes within a fixed casing. The rotors are carefully shaped to ensure that lines of continuous contact occur between the rotors. This combined with the small clearance gap between the rotor tips and the stationary casing creates a series of separate working chambers. The volume of a working chamber enclosed within the two rotors and the side and end faces of the casing is seen to vary with the angular position of the rotors. Carefully shaped holes, or ports, in the end faces of the casing then allow fluid to enter and leave the working chambers once specified volumes are reached, allowing either compression or expansion of the fluid passing through the machine.

An alternative configuration for positive displacement machines involves internally geared rotors. These can be used in various configurations of pump, either as straight cut rotors (such as gerotor or internal lobe pumps) or as helical rotors with open ends (such as progressive cavity pumps). An important feature of the rotor profiles is the requirement for continuous contact between rotors. Details of rotor profile generation for such applications are described by Colbourne (1974), Beard (1988), Beard et al. (1992), Vecchiato et al. (2001) and Litvin & Fuentes (2004). Moineau (1932) appears to have been the first to describe how the geometry of such rotors can be defined and proposes the use of rotors with variable pitch or variable profile in order to achieve a change in the volume of the working chamber between inlet and discharge of the machine. More recent developments have looked at implementing the concept of conical internally geared rotors for a range of compressor applications (Dmitriev et al., 2015). There are considerable challenges in manufacturing rotors of this type with the requisite high accuracy using efficient and economical methods, and a simpler configuration using constant pitch and profile rotors with stationary porting has been previously proposed by the authors (Read et al. 2017). This paper aims to investigate the influence of port flows on the isentropic efficiency of such machines.

2. OVERVIEW OF MACHINE GEOMETRY

2.1 Rotor Profiles

Internally geared positive displacement machines require continuous contact points between inner and outer rotors during rotation about parallel axes. This allows the formation of enclosed working chambers whose volume varies with the angular position of the rotors. A wide range of rotor profiles can be generated that meet this requirement. In this paper, simple geometries consisting of epicycloids and hypocycloids are used to illustrate this requirement of continuous contact between rotors and to investigate machine performance. These profiles require that the inner rotor has one fewer lobe than the outer rotor. The equations defining coordinates of epicycloid and hypocycloid profiles are shown in Equation 1. While cycloids are used in this paper to illustrate the analysis of internally geared machines, it should be noted that there is considerable scope for optimization using other methods of rotor profile generation.

$$\begin{bmatrix} x_e(\theta) \\ y_e(\theta) \end{bmatrix} = \begin{bmatrix} (r_b + r_e)\cos\theta - r_e\cos\big(\theta(r_b/r_e + 1)\big) \\ (r_b + r_e)\sin\theta - r_e\sin\big(\theta(r_b/r_e + 1)\big) \end{bmatrix}$$

$$\begin{bmatrix} x_h(\theta) \\ y_h(\theta) \end{bmatrix} = \begin{bmatrix} (r_b - r_h)\cos\theta + r_h\cos\big(\theta(r_b/r_h - 1)\big) \\ (r_b - r_h)\sin\theta - r_h\sin\big(\theta(r_b/r_h - 1)\big) \end{bmatrix} \quad (1)$$

Continuous contact between rotors can be achieved using composite profiles which can be created by combining sections of epicycloid and hypocycloid profiles. The profiles are defined by the radius of the base circle, r_b, the number of lobes required on the rotor, N, and the radius of the epicycloid generating circle, r_e, where $0 < r_e < r_b/N$. By considering the circumferences of the epicycloid and hypocycloid generating circles, it can be seen that the radius of the hypocycloid generating circle, $r_h = r_b/N - r_e$. In order to achieve the required meshing condition between the inner and outer rotors it can be shown r_e and r_h must be equal for both rotors, and that the relationship in Equation 2 must be true, where E is the distance between the rotor axes. This allows a normalized rotor profile parameter, λ, to be defined as shown.

$$r_e/E = r_e/(r_e + r_h) = \lambda \quad (2)$$

It is clear from Equation 2 that the possible values of the ratio λ range between zero and one, corresponding to the cases when the rotors are pure hypocycloids and epicycloids respectively. Examples of different rotor profiles are shown in Figure 1, where the value of E has been scaled in each case in order to achieve the same maximum profile diameter.

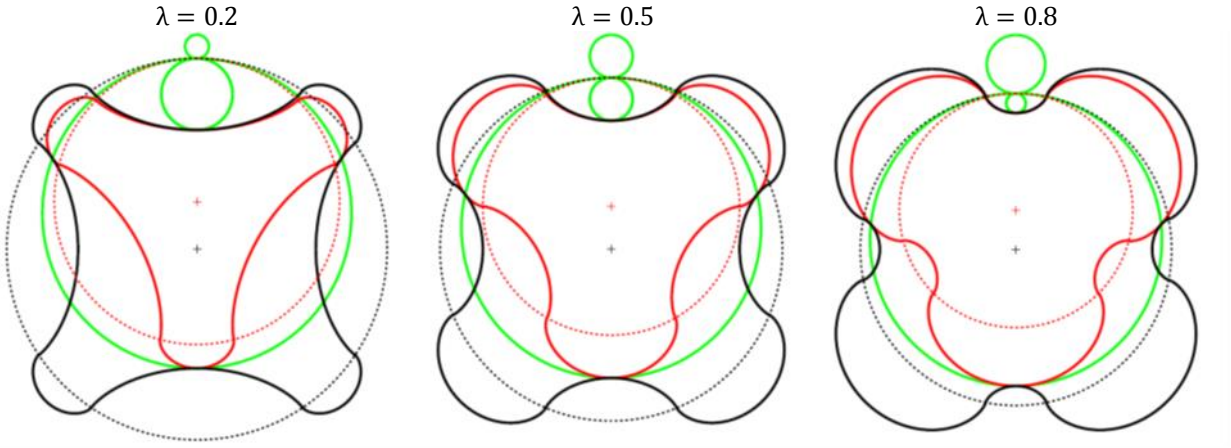

Figure 1: Inner (red) and outer (black) rotor profiles for values of $\lambda = 0.2, 0.5$ and 0.8, showing loci of contact points during rotation (green) and rotor pitch circles (dotted lines)

2.2 Screw Geometry

Once the rotor profiles have been specified the contact points can be identified using the meshing condition for the two rotors. This states that the normal to the surface of both rotors at a point of contact must pass through the pitch point of the rotors, which is the point where the base circles of the inner and outer rotors coincide. The area contained between two rotor contact points can then be characterised as a function of the angular position of the rotor profiles. This working chamber area is seen to increase from zero (at the angular position where two contact points converge) to a maximum value. Due to the symmetry of the rotor lobes, the working chamber area as a function of angular position is symmetrical about this point of maximum area, as illustrated in Figure 2.

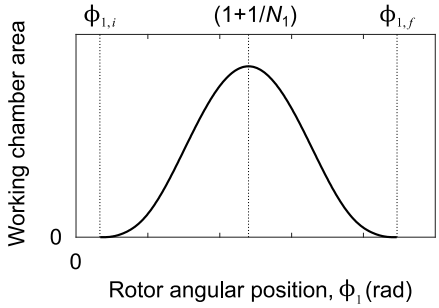

Figure 2: Illustration of working chamber area as function of angular position

For helical rotors at a fixed angular position, the variation of area with profile angular position can be related to the cross-sectional area of the working chamber as a function of longitudinal location. As for conventional screw machines, this requires the wrap angle of the rotors, Φ, to be defined along with the rotor length, L (Stosic, 2005). Hence, for a specific rotor position, the volume of the working chamber can be found by performing an integration of the area w.r.t. the longitudinal coordinate, z. Alternatively, the integral can be performed w.r.t the rotor angular position, ϕ_1., where the cross-sectional areas of the working chamber at the two end faces of the rotors can be used to determine the volume as illustrated in Figure 3 and defined in Equation 3. Note that as the rotors have constant pitch, $dz/d\phi_1 = L/\Phi_1$. The working chamber volume can therefore be found as a function of rotor position.

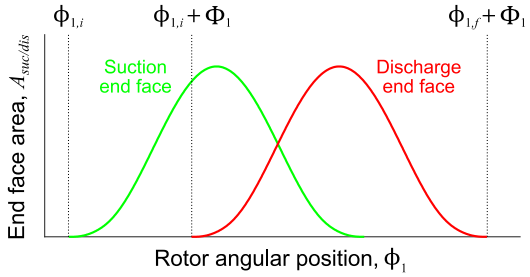

Figure 3: Illustration of working chamber volume calculation by integration w.r.t. angular position

$$V_{wc} = \int_0^L A_{wc}\,dz = \frac{L}{\Phi_1}\int_{\phi_{1,i}}^{\phi_1} (A_{suc} - A_{dis})\,d\phi_1 \tag{3}$$

When considering the helix wrap angle, it is clear from Figure 3 that if $\Phi_1 \geq (\phi_{1,f} - \phi_{1,i})$, then a working chamber is never exposed to both end faces at the same time. In a compressor application this means that the working chamber will not be exposed to the suction end face when the volume reaches maximum or during the following compression process, hence this face can be completely exposed to the low pressure supply. If $\Phi_1 < (\phi_{1,f} - \phi_{1,i})$ then there will be some exposure of the working chamber to the suction end face when the volume reaches maximum, and a shaped port is therefore necessary to close the working chamber for the low pressure supply at this point. As $\phi_{1,i}$ and $\phi_{1,f}$ depend on the rotor profiles, it is useful to consider a normalized rotor wrap angle, $\bar{\Phi}_1$, as defined in Equation 4, in order to compare the performance of different configurations.

$$\bar{\Phi}_1 = \Phi_1/(\phi_{1,f} - \phi_{1,i}) \quad (4)$$

In order to achieve positive displacement of the working fluid using constant pitch and profile rotors, porting is necessary to close the working chamber from the suction end at the angular position when maximum volume is reached, and open the working chamber to the discharge once the specified compression has occurred. The built-in volume ratio (ϵ_v) of the machine is the ratio of the maximum working chamber volume to the minimum volume at which the working chamber remains closed from either the suction or discharge ports. The volume vs. rotor position curve for a particular machine configuration allows the geometry of the suction and discharge ports to be defined in order to achieve a particular value of ϵ_v. This is achieved by identifying the position of the rotor profiles at the discharge (high pressure) end face of the rotors at the point where the working chamber volume reaches the required value. These profiles are then used along with the loci of contact points to define a port area which ensures that flow can only enter or leave the working chamber once the required position is reached.

Similarly, the suction (low pressure) end face of the working chamber can be found at the point of maximum working chamber volume. The maximum port area is found using these rotor profiles and the contact loci line projected a the low pressure end face. If the wrap angle of the rotors is sufficient to create a working chamber that is completely enclosed by rotor-to-rotor contact lines (i.e. $\bar{\Phi}_1 \geq 1$), then the suction end face can be completely open without affecting the maximum volume of low pressure fluid in the machine. The construction of the port geometry and the calculation of flow area for both the suction and discharge ports are illustrated in the following section.

2.3 Calculation of Port Flow Areas

The suction and discharge port flow areas are found by considering the overlapping area between the port opening and the end face of the working chamber. Figure 4 illustrates a general case of port geometries with helical rotors. The ports follows the rotor profiles at the positions where suction ends and discharge commences, and contact point loci in order to ensure no opening of the working chamber to either suction or discharge occurs during compression. Note that in this case where $\bar{\Phi}_1 < 1$ there is some region of the suction end face that must be covered. Increasing the wrap angle increases the suction port area (up to a maximum area at $\bar{\Phi}_1 = 1$), while also increasing the discharge port area. Increasing the built-in volume ratio for a given wrap angle has no effect on the suction port, but reduces the discharge port area, as the volume must be reduced further before the port can open.

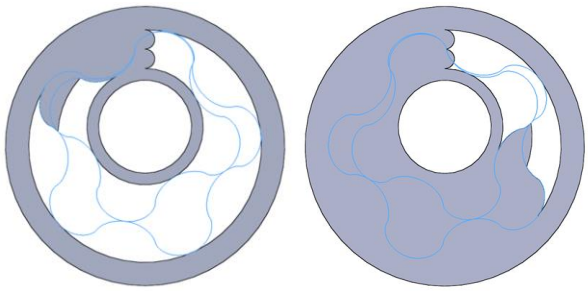

Figure 4: Illustration of suction and discharge port areas for case with $\lambda = 0.5$, $N_1 = 5$ and $0 < \bar{\Phi}_1 < 1$

Once the port areas are defined, it is possible to apply a calculation procedure to find the area of overlap between the ports and the exposed areas of the working chamber at each end face (as shown in Figure 3). This allows the flow area at each port to be found. An example of the effect of wrap angle and built-in volume ratio on the volume and flow areas for the helical internally geared machines is shown in Figure 5. The higher maximum working chamber volume is achieve using the lower value of $\bar{\Phi}_1$, although this requires the suction port to close sooner, and results in slightly lower maximum discharge port areas. The results in Figure 5 suggest that the main difference in port flow for the cases shown with $\bar{\Phi}_1 = 0.5$ and 1 is likely to be due to the difference in $dV/d\phi_1$ rather than differences in the port flow areas.

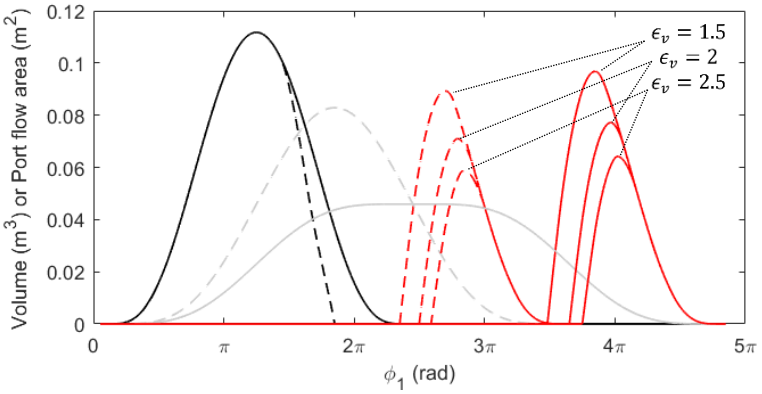

Figure 5: Illustration of suction (black line) and discharge (red line) port flow areas and working chamber volume (grey line) for rotor profile $\lambda = 0.8$. Dashed and solid lines show cases when $\bar{\Phi}_1 = 0.5$ and 1 respectively

2.4 Calculation of Leakage Areas

Inter-lobe leakage areas can be calculated by tracking the contact points in order to find the length of sealing lines connecting the working chamber being considered with other working chambers. These leakage line lengths are function of the rotor profiles, the length and maximum diameter of the rotors and the wrap angle. The length of the line connecting to individual working chambers needs to be tracked in order to apply the correct pressure and temperature conditions for each leakage flow to or from the working chamber being considered. The end face leakage areas can be estimated by simply considering the perimeter of the end faces of the working chamber when exposed to the suction and discharge ends of the rotors, as illustrated in Figure 3. These perimeter lengths are again functions of the rotor profile and maximum diameter and wrap angle. Future work will focus on the effect of these leakage flows during the filling, compression and discharge processes.

3. SCREW MACHINE PERFORMANCE ANALYSIS

3.1 Calculation procedure

A simple model of oil free air compressor has been developed in order to investigate the effect of the port flow and leakage on the performance of internally geared machines. Matlab/Simulink software has been used to calculate the solution of the differential equation describing conservation of internal energy for a single working chamber:

$$\omega_1 \left(\frac{dU}{d\phi_1}\right) = \dot{m}_{in} h_{in} - \dot{m}_{out} h_{out} + \dot{Q} - \omega_1 p_{wc} \left(\frac{dV_{wc}}{d\phi_1}\right) \tag{5}$$

In the current analysis the heat transfer term is neglected. The geometry of the machines has been generated as described in the previous section. Once values of λ, N_1, $D_{1,max}$, L and $\bar{\Phi}_1$ have been specified, the following variables can be defined as functions of the rotor position, ϕ_1:

- Working chamber volume, V_{wc}
- Suction and discharge port flow areas, A_{suc} and A_{dis}
- Perimeter length of working chamber on rotor end faces, l_{suc} and l_{dis}
- Length of inter-lobe sealing lines between working chambers, l_{seal}

The mass flow rates into and out of the working chambers via the ports and leakage paths therefore need to be characterized in order to solve Equation 5.

3.2 Port Flow and Leakage Model

The flow of gas through port and leakage paths has been modelled using simple valve mass flow rate equations, with the valve flow coefficient assumed to be proportional to flow area. The mass flow rate of the gas, $\dot{m}$, is calculated using the following equations, where the subscripts *h* and *l* refer to conditions on the high and low pressure sides of the valve respectively:

If $p_l \geq p_h/2$ $\qquad \dot{m} = C_v N p_h \rho_{stnd} \left(1 - \frac{2(p_h - p_l)}{3p_h}\right) \sqrt{\frac{(p_h - p_l)}{p_h T_h}}$

$$\text{If } p_l < p_h/2 \qquad \dot{m} = 0.471\, C_v N p_h \rho_{stnd} \sqrt{1/T_h} \tag{6}$$

Using SI units, the value of $N = 1.158 \times 10^{-6}$, and ρ_{stnd} is the density of air at standard conditions. The valve coefficient is estimated as $C_v(\phi_1) = K_v A$, where K_v is a constant of proportionality and A is the flow area. These equations can be applied to the suction and discharge port flow areas, A_{suc} and A_{dis}. They can also be applied to the various leakage path in the machine. The end face leakage areas can be found by multiplying the perimeter lengths (l_{suc} and l_{dis}) by an axial clearance between the rotor end faces and the housing, C_{ax}. The inter-lobe leakage areas can be estimated by multiplying the chamber-to-chamber sealing line lengths by a radial clearance, C_{rad}.

3.3 Machine Performance Results

A number of machine geometries have been considered using the following parameter values:

Parameter		Value(s)
Outer rotor lobes	N_1	4
Outer rotor length/diameter ratio	$L/D_{1,max}$	1
Rotor profile parameter	λ	0.2, 0.4, 0.6, 0.8
Machine volume ratio	ϵ_v	1.5, 2, 2.5
Normalised outer rotor wrap angle	$\bar{\Phi}_1$	0.25, 0.5, 1

It should be noted that the area of the low pressure suction port, $A_{suc}(\phi_1)$, is only a function of the rotor profile, ρ_e/E, and the wrap angle, $\bar{\Phi}_1$, while the high pressure discharge port also depends on the machine volume ratio, ϵ_v.

A fixed length-to-diameter ratio, $L/D_{1,max} = 1$, is used in the analysis. For a given machine geometry, changing the rotor length will result in a proportional change to the maximum volume of the working chamber. The port areas and end faces leakage areas will remain the same, but the inter-lobe leakage areas will vary in proportion to the length of the rotor tip, $l_{1,tip}$, where:

$$l_{1,tip} = \sqrt{L^2 + \left(\phi_1 D_{1,max}/2\right)^2} \tag{7}$$

The effect of $L/D_{1,max}$ on the machine performance will be considered in future work.

The effect of rotor profile, wrap angle and built-in volume ratio have been investigated by calculating the isentropic and volumetric efficiency of the different geometries. In this initial analysis, the discharge pressure is set to equal that achieved by the machine assuming an ideal cycle, with no losses during filling and emptying of the working chamber (i.e. no pressure difference across suction and discharge ports), and an adiabatic compression process for the specified volume ratio. Hence the discharge pressure is set equal to $p_{dis,adi}$, where:

$$p_{dis,adi} = p_{suc}(\epsilon_v)^{\gamma} \tag{8}$$

In order to investigate the effects of the port flow areas on efficiency, the axial and radial clearance values were initially set to zero for a 'no leakage' case. The results in Figure 6 show how the working chamber pressure varies with angular position for a range of volume ratios and wrap angles; in all cases the rotor profiles and the rotational speed are the same. It is clear that the smaller wrap angle results in larger pressure differences across both the suction and discharge ports. This is due to both the larger maximum working chamber volume and the smaller port areas (and hence flow areas) that are possible. The pressure difference across the discharge port is seen to increase with the volume ratio, again reflecting the reduced discharge port flow area possible with higher compression ratio.

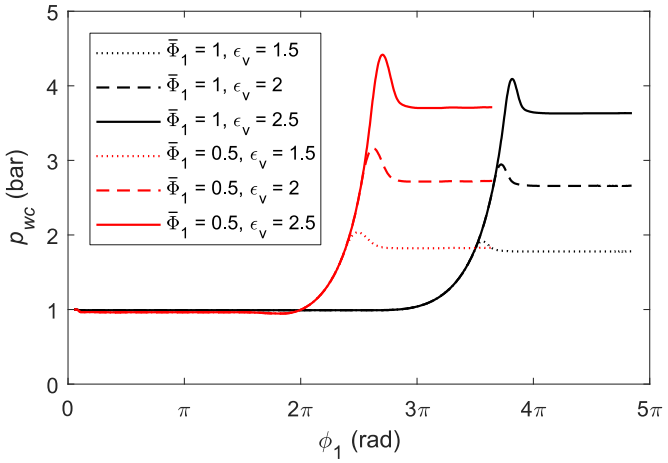

Figure 6: Working chamber pressure for machines with $\lambda = 0.8$ and the specified values of ϵ_v and $\bar{\Phi}_1$, assuming no leakage losses ($p_{suc} = 1bar$, $p_{dis} = p_{dis,adi}$, $v_{tip,max} = 100m/s$)

The isentropic efficiency of the machines shown in Figure 6 has been calculated by comparing the integral of the pressure-volume curve for these cases with the work required in the ideal adiabatic compression cycle. This has been performed for a range of rotational speeds. These results are shown in Figure 7. It is clear that the higher pressure difference across the ports for the case with lower wrap angle leads to higher losses, hence a lower isentropic efficiency. The isentropic efficiency is seen to increase with built-in volume ratio, as even though a larger pressure difference is required during discharge, this additional compression work is a lower proportion of the overall compression work. In all cases the efficiency is seen to decrease with increasing rotational speed, which is to be expected due to the higher mass flow rate that will occur through the same port flow areas.

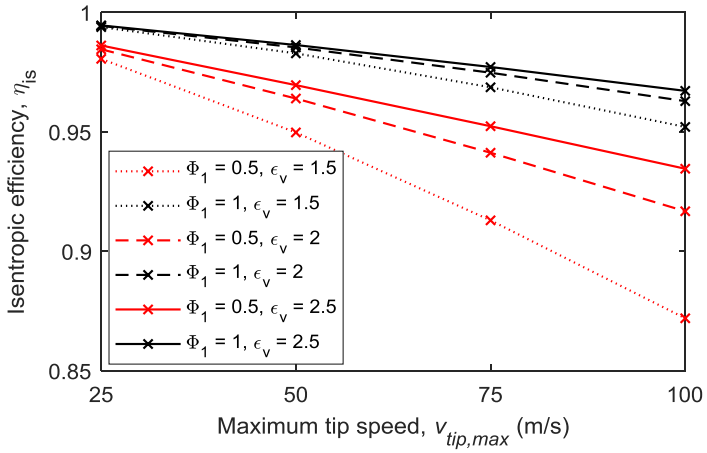

Figure 7: Isentropic efficiency for machines with $\lambda = 0.8$ and the specified values of ϵ_v and $\bar{\Phi}_1$, assuming no leakage losses ($p_{suc} = 1bar$, $p_{dis} = p_{dis,adi}$)

The performance of machines with different rotor profiles has also been considered. Figure 8 shows the calculated isentropic efficiency for machines with the same volume ratio and normalized wrap angle, but with different values of λ. The isentropic efficiency is seen to increase with λ, suggesting that epicycloid type profiles can achieve lower port flow losses, although a range of other factors including the influence of leakage losses also need to be considered.

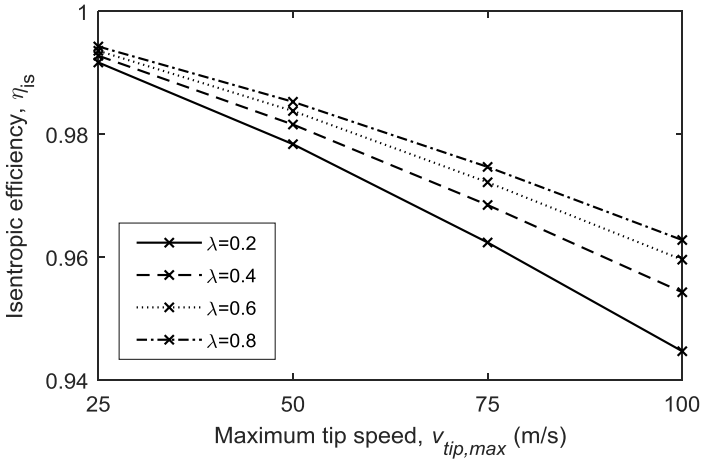

Figure 8: Effect of rotor profile on isentropic efficiency for machines with $\epsilon_v = 2$ and $\bar{\Phi}_1 = 1$, assuming no leakage losses ($p_{suc} = 1bar$, $p_{dis} = p_{dis,adi}$)

In order to investigate the influence of the discharge pressure on the machine performance, it has been varied for the cases shown in Figures 6 and 7. The results in Figure 9 illustrate that the discharge pressure that results in maximum isentropic efficiency for a given machine geometry is higher than that resulting from the ideal adiabatic compression cycle. For the cases with the larger wrap angle ($\bar{\Phi}_1 = 1$), the optimum discharge pressure was found to be 20-30% higher than $p_{dis,adi}$, while for the lower wrap angle ($\bar{\Phi}_1 = 0.5$) it was 40-50% higher than $p_{dis,adi}$. At these optimum discharge pressures, the machines with the lower wrap angle were again found to have lower isentropic efficiencies

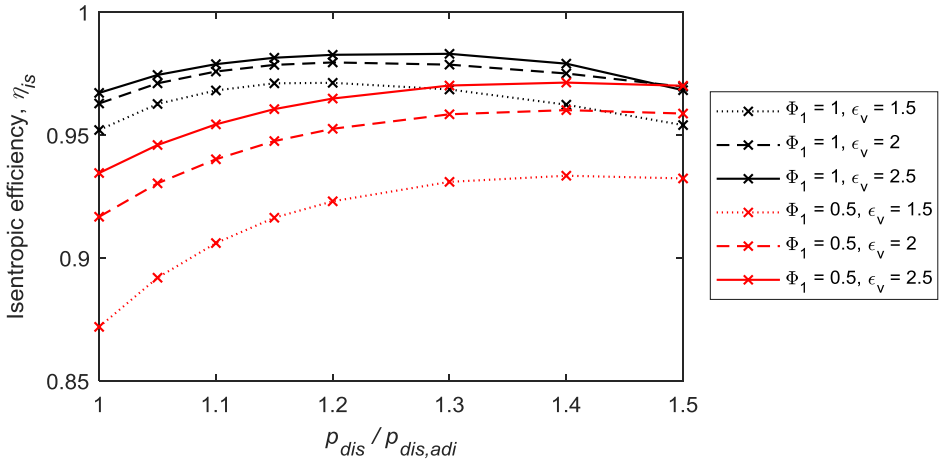

Figure 9: Effect of discharge pressure on isentropic efficiency for machines with $\lambda = 0.8$ and the specified values of ϵ_v and $\bar{\Phi}_1$, assuming no leakage losses ($p_{suc} = 1bar$, $v_{tip,max} = 100m/s$)

4. CONCLUSIONS

This paper has investigated the effect of various geometrical parameters on the performance of internally geared screw machines. The losses that occur during filling and discharge of the machine are primarily dependent on the rate of change of volume, $dV/d\phi_1$, and the flow area. The main conclusions from the study are as follows:

- For screws with specific profiles and wrap angles in the range $0.5 < \bar{\Phi}_1 < 1$ the maximum port areas are similar, and the filling and discharge losses are dominated by $dV/d\phi_1$.
- For a specific profile and wrap angle, isentropic efficiency was found to increase with built-in volume ratio over the range $1.5 < \epsilon_v < 2.5$
- For a specific normalized wrap angle and volume ratio, the isentropic efficiency was found to increase with λ, meaning that profiles closer to a pure epicycloid achieved lower losses due to port flow.
- The performance of the screw machines is sensitive to the discharge pressure, which should be optimized in order to achieve maximum isentropic efficiency for a given volume ratio.

In reality, the discharge pressure for a particular application is likely to be fixed, and ϵ_v should then be optimized along with geometry and rotational speed to achieve the best performance. Future work will focus on integrating the calculation of the port areas with the main compressor model in order to implement this type of multi-variable optimization. Further work is also required to better characterize the relationship between area and mass flow rate both for the ports and the leakage paths, and to develop the model to include oil-injected operation.

NOMENCLATURE

A	area	(m^2)
E	distance between rotor axes	(m)
L	rotor length	(m)
N	number of lobes on rotor	(–)
p	pressure	(bar)
V	volume	(m3)
ρ	diameter	(m)
ϕ	angular position of rotor	(rad)
Φ	wrap angle of rotor	(rad)
ω	angular speed	(rad/s)
θ	cycloid generating angle	(rad)
ϵ_v	built-in volume ratio	(–)
λ	Rotor profile parameter	(–)

REFERENCES

Colbourne, J.R. (1974). The geometry of trochoid envelopes and their application in rotary pumps. Mechanism and Machine Theory, 9(3-4), pp.421-435.

Beard, J.E. (1985). Kinematic analysis of gerotor type pumps, engines, and compressors, PhD thesis.

Beard, J.E., Yannitell, D.W. and Pennock, G.R. (1992). The effects of the generating pin size and placement on the curvature and displacement of epitrochoidal gerotors. Mechanism and Machine Theory, 27(4), pp.373-389.

Vecchiato, D., Demenego, A., Argyris, J. and Litvin, F.L. (2001). Geometry of a cycloidal pump. Computer methods in applied mechanics and engineering, 190(18), pp.2309-2330.

Litvin, F.L. and Fuentes, A. (2004). Gear geometry and applied theory. Cambridge University Press.

Moineau, R.J.L. (1932). Gear mechanism. U.S. Patent 1,892,217.

Dmitriev, O., Tabota, E., and Arbon, I. (2015). A miniature Rotary Compressor with a 1:10 compression ratio. In IOP Conference Series: Materials Science and Engineering. Vol. 90. No. 1. IOP Publishing.

Read, M. G., Smith, I. K., & Stosic, N. (2017). Internally geared screw machines with ported end plates. In IOP Conference Series: Materials Science and Engineering. Vol. 232, No. 1, p. 012058. IOP Publishing.

Stosic, N., Smith, I. and Kovacevic, A. (2005). Screw compressors: mathematical modelling and performance calculation. Springer Science & Business Media.